# Fatigue Studies of Titanium Alloys Used For Aero Engines

***Dissertation submitted to***
***Visvesvaraya National Institute of Technology, Nagpur***
***in partial fulfilment of the requirements for the award of***
***the degree***

## Master of Technology

## in

## Materials Engineering

***by***


**AKSHAY ANAND MHAISKE**

**(MT23MTE001)**


under the guidance of

**Dr. M. M. Thawre** **Dr. A. R. Ballal**

**Department of Metallurgical & Material Engineering**

**Visvesvaraya National Institute of Technology**

**Nagpur 440010 (India)**


**June 2025**


©Visvesvaraya National Institute of Technology (VNIT) 2025

# Department of Metallurgical & Material Engineering

# Visvesvaraya National Institute of Technology, Nagpur

## Declaration

I, Akshay Anand Mhaiske hereby declare that this dissertation titled "**FATIGUE STUDIES OF TITANIUM ALLOYS USED FOR AERO ENGINES**" is carried out by me in the Department of Metallurgical & Material Engineering of Visvesvaraya National Institute of Technology, Nagpur. The work is original and has not been submitted earlier in whole or in part for the award of any degree/diploma at this or any other Institution / University.

Akshay Anand Mhaiske

20 May 2025

## Certificate

This is to certify that the dissertation titled **"FATIGUE STUDIES OF TITANIUM ALLOYS USED FOR AERO ENGINES"** is submitted by **Akshay A Mhaiske** in partial fulfilment of the requirements for the award of the degree of **Master of Technology** in **Materials Engineering** VNIT, Nagpur. The work is comprehensive, complete, and fit for final evaluation.

Dr. M. M. Thawre
Associate Professor

Dr.A.R.Ballal
Professor

Dr.D.R.Peshwe
(Head of Department)

**VISVESVARAYA NATIONAL INSTITUTE OF TECHNOLOGY**

**NAGPUR**

# Non – Plagiarism Certificate

This is to be certified that M.Tech Dissertation titled "**Fatigue Studies of Titanium Alloys used for Aero Engine**s" submitted by **Akshay Anand Mhaiske**, Enrollment No.MT23MTE001, ID No. **30819** has been checked plagiarism using TURNITIN Software and the overlap is found within prescribed limits. A summary of the report is given below,

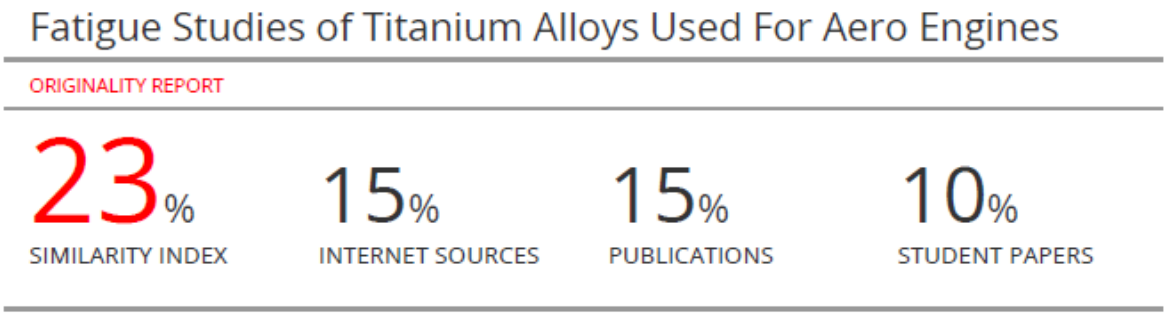


Sign:

**Name: Akshay Anand Mhaiske**

Enrollment No: MT23MTE001

ID No: 30819

**Dr. M. M. Thawre**
Associate Professor,
Department of Metallurgical & Materials Engineering
VNIT, Nagpur

**Dr.A.R.Ballal**
Professor,
Department of Metallurgical & Materials Engineering
VNIT, Nagpur

# ACKNOWLEDGEMENT

I would like to take the privilege to express gratitude and respect to all those who helped me in completion of this project work.

I am very much delighted to express my sincere gratitude to my **Guide, Dr. M. M. Thawre and Co-Guide Dr. A. R. Ballal, Professor** Department of Metallurgical and Material Engineering, VNIT-Nagpur, for their encouragement and support that they extended towards me during this project work.

I specially acknowledge them for their advice, supervision, and the vital contribution as and when required during this research. Their involvement with originality has triggered and nourished my intellectual maturity that will help me for a long time to come. I am proud to record that I had opportunity to work with an exceptionally experienced Professors like them.

I would like to thank **Dr. D. R. Peshwe, Head of Department**, Department of Metallurgical and Material Engineering VNIT-Nagpur for support during this project.

Special thanks are due to Vivek, Patankar madam, Prasanna, Pramod, Priyanshu, Apurwa for their continuous support and help throughout the course of my project.

Finally, yet importantly, I would like to express my heartfelt thanks to my beloved parents and sister for their blessings and my batch mates for their help and wishes for the successful completion of the project.

# ABSTRACT

Ti64 comes under the category of nonferrous and light metal alloy known as (α+β alloy). Due to its unique physical, chemical and mechanical properties like high strength to weight ratio and resistance to corrosion makes it a choice as an aeronautical industry's favorable alloy. It has an exceptional application in gas turbine fan compressor, and aircraft structural parts that are exposed to high temperature during service condition. A constant amplitude fatigue behavior of Ti64 at room temperature (RT) and 150 °C was studied. Experiments were conducted to determine the high cycle fatigue strength of Ti64 alloy at room temperature (RT) and at moderately elevated temperature (150 °C) at a stress ratio (R) of 0.5. Based on the yield strength (Y.S.) of the material the test matrix has been designed. The tests were conducted from minimum 600 MPa to maximum yield strength of the material at incremental stress of 50 Mpa. Hour glass specimens as per ASTM E 466 with gauge diameter of 6 mm were tested at constant frequency (say 77 Hz) on RUMUL TESTRONIC resonance machine (100 kN capacity). The results indicate that fatigue strength tends to decline as the temperature rises. Specifically, at 150 °C, this reduction is likely caused by factors such as thermal softening, higher dislocation mobility, oxidation, and changes in the material's microstructure. Fractographic investigations were carried out on failed specimen. Results show that the specimen at room temperature failed due to primary crack which originated from surface while for moderately elevated temperature (150 °C) multiple crack initiation sites were observed on the surface.

# CONTENTS

**Chapter 1: Introduction……..1**

Introduction of Ti64 alloy……..1

Kaveri Engine Programme……1

Ti64 (α+β Titanium alloy)…….....2

Objective……3

Organisation of thesis……3

**Chapter 2: Literature review …..…….…..... 4**

Literature review……...….4

Research gap…….…..…6

Fundamentals of fatigue ……....6

High cycle fatigue ……....6

Fatigue limit ……..…6

S-N curve …….….7

Fatigue test parameters ……7

Types of cyclic loading ……..…8

Variable loading…….…8

Block loading……....9

Fracture ……....10

Crack initiation ……10

Crack propagation …….…. 11

Final fracture……11

Ductile fracture……12

Brittle fracture……..12

Failure mode……13

Fatigue failure……..14

**Chapter 3: Experimental detail …...…….16**

Material: Ti64 alloy…….....16

Specimen details……..16

Test matrix……17

Methodology adopted……..17

Equipment used …….. 18

RUMUL testing machine ……... 18

Testing methodology …….. 20

EDM machine …… 20

Hot mounting machine …..……. 20

Polishing machine …….. 21

Etching …….. 22

Optical microscope …… 22

Scanning electron microscope (SEM) …… 23

Vickers micro hardness …….……..... 24

**Chapter 4: Results and discussion …...……25**

Fatigue results test matrix……..…… 25

S-N curve …….…….…..... 26

Microstructure ……26

Fractography……29

Vickers micro hardness ……..... 32

**Chapter5: Conclusion ……..... 33**

**Scope of future research……34**

**References ……..35**

# LIST OF FIGURES

Figure 2.1 Fatigue S-N curves ……. 7

Figure 2.2 Types of stress cycles in fatigue load a) Reversed stress b) Repeated stress c) Random stress …….. 8

Figure 2.3. Applied Block loads…….10

Figure 2.4. Formation of slip bands as extrusions and intrusions ……...11

Figure 2.5 a) Failure by localised plastic without necking b) Failure by localised plastic with necking c) Failure by void coalescence with obvious necking ……..12

Figure 2.6. Modes of crack formation……. 14

Figure 3.1. Geometric drawing and picture of High cycle fatigue hour glass specimen as per ASTM E 466 ……...……17

Figure 3.2. Showing the Experimental Flow Chart Analysis details of fatigue tested specimen

…….18

Figure 3.3. RUMUL High Cycle Fatigue (HCF) testing machine……..……19

Figure 3.4. Electro discharge machine (EDM) machine…….....20

Figure 3.5. Hot mounting machine …….21

Figure 3.6. Polishing machine …… ……22

Figure 3.7. Optical metallurgical microscope …… 23

Figure 3.8. Scanning electron microscope ……..... 24

Figure 3.9. Vickers micro hardness testing machine …….. 24

Figure 4.1. S-N Curve for Ti64 alloy ……..……...……...…. 26

Figure 4.2. A as-received Ti64 alloy showing optical microstructure (a, b,) at 100x, 200x,)…….. 27

Figure 4.3. SEM structures showing the in-depth morphology of as received specimen….……...….. 27

Figure 4.4. Microstructure of cyclically failed specimen ……..…….…… 28

Figure 4.5.A. SEM Fractrograph showing the in-depth morphology of the fracture……29

Figure 4.5.B. SEM Fractrograph showing the in-depth morphology of the fracture……....30

Figure 4.6: SEM structure showing EDS mapped region…….32

Figure 4.7: EDS graph showing elemental peak……...32

Figure 4.8. Hardness Profile of as received specimen and tested samples……33

# LIST OF TABLES

Table 1.1 Constant physical properties of Ti64alloy……..……2

Table 3.1. Chemical composition of Ti64alloy …….…..16

Table 3.2: Test matrix of Ti64 Alloy…….…...17

Table 4.1: Fatigue test results of Ti64 Alloy……25

# Chapter 1

## INTRODUCTION

In this chapter introduction about titanium alloy, project objectives, Kaveri engine programme brief discussion, & organisation of thesis are presented.

## 1.1 Introduction of Ti64 alloy

Ti64 alloy commonly referred to as Grade 5 Titanium alloy, is a widely utilized material in aerospace industry due to its exceptional combination of high strength to weight ratio, excellent corrosion resistance and remarkable mechanical properties. It contain 90% titanium, 6% aluminium, and 4% vanadium, with aluminium stabilizing the alpha phase (α) and vanadium stabilizing the beta phase (β), resulting a two-phase (α+β) microstructure. This unique structure provides a balanced blend of strength, toughness, and ductility, making Ti64 ideal for critical aeronautical engine components.

In aeronautical engines, materials are subjected to extreme temperatures, high cyclic loads, and aggressive environmental conditions. Ti64 is ideal for components such as compressor blades, fan discs, casings, landing gears and fasteners, where its high tensile strength (up to 1150 MPa) and low density (4.43 $g/cm^3$) contribute to enhanced efficiency and reduced overall engine weight. Moreover, its ability to withstand temperature up to 400 °C without significant loss of mechanical properties ensures reliability during high speed rotations and thermal cycling.

This introduction aims to explore the high cycle fatigue behaviour of Ti64 alloy, with a focus on its application in aero engine components. Key factors such as fatigue strength, microstructural optimization, and stress analysis are discussed to highlight the alloy's capability in sustaining long term cyclic loads.

## 1.2 Kaveri Engine Programme

The Kaveri Engine programme was initiated in 1980s, it aimed to reduce India's dependence on foreign propulsion system for its fighter jets. It is running under Gas Turbine Research Establishment (GTRE), a lab under the Defense Research and Development Organization

(DRDO) of India to develop an indigenous gas turbine jet engine for powering military aircraft, particularly the Tejas Light Combat Aircraft. The material is produced in 40 mm Ø in hot rolled condition and further annealing is done to improve its machinability. Design goal is to develop a low-bypass turbofan engine 80-90 kN thrust class with afterburner.

## 1.3 Ti64 (α+β Titanium alloy)

It is composed of three major elements mainly titanium, aluminum and vanadium along with iron, molybdenum, with some amount of oxygen, nitrogen, carbon.

Aluminum(Al): The role of Al is to stabilize the alpha (α) phase, which is the hexagonal close-packed (HCP) structure which increases strength, improved creep resistance, reduce density and improve surface oxidation resistance.

Vanadium (V): The role of V is to stabilize the beta (β) phase, which is body-centered cubic (BCC) structure which enhanced ductility and formability, increased strength and Toughness of the material.

Minor Elements and Trace Impurities:

Iron (Fe): Fe improves strength slightly due to solid solution strengthening, it is kept at low levels typically ≤ 0.25% to avoid excessive brittleness.

Oxygen: O increases strength but reduces ductility.

Nitrogen: N adds strengths similarly to O but can also reduce toughness if concentration is too high.

Carbon: C contributes marginally to hardness and strength, it is kept below 0.08 % to avoid embrittlement.

Hydrogen: High hydrogen levels can lead to embrittlement, so it is carefully controlled (≤ 0.015)

Table 1.1 Constant physical properties of Ti64 alloy

| | |
|---|---|
| Density ($Mg/m^3$) | 4.43 |
| Melting Range (°C) | 1604-1660 |
| Specific heat at 26°C | 0.52 J/Kg °C |

## 1.4 Objectives:

- Study of the High Cycle Fatigue (HCF) behavior of Ti 64 alloy
- Generation of fatigue data for Stress ratio (R) = 0.5 at RT and 150$^{o}$C

## 1.5 Organisation of thesis

- Chapter 2 presents detailed literature review covering the work done by various researchers on Ti64 and fundamentals of fatigue.
- The methodology adopted for evaluation of fatigue behaviour of Ti 64 at RT & 150 $^{\circ}$C is given in chapter 3. Details about material and specimen preparation are also covered here. Various sophisticated characterization techniques were used for studying the failure features of fatigue tested specimens.
- Detail results on microscopic studies before and after fatigue tests, fractography of failed specimens and fatigue data generated for two temperatures are elaborated in chapter 4, results and discussion.
- Chapter 5 gives the conclusion drawn based on the research work carried out followed by references.

# Chapter 2

# LITERATURE REVIEW

In this chapter basics of fatigue and literature on Fatigue of Ti64 is presented in depth, it deals with various types of microstructure their effect on fatigue limit, various stress ratio effects on fatigue strength, different frequency used to test the material and their effect are discussed

**Zhihong Wu** investigated HCF behaviour of Ti-6Al-4V alloy at RT and 400 °C. The work is done on forged plate of Ti64 with various heat treatment**.** He obtained 4 types of microstructure by adjusting post-forging heat treatment processes. Stress-controlled HCF tests were performed according to Chinese standard/T 3075-2008. Stress ratio R= -1 was used at a frequency of 120 Hz. The test end criteria was specimen failure completely or achieved $10^7$ cycles or say run-out. Results showed that fatigue strength monotonically increased with increasing primary-α ($\alpha_p$) percentage for RT specimen. Moderate $\alpha_p$ percentage showed slightly higher fatigue strength value at 400 °C. 40-60% $\alpha_p$ exhibited relatively longer fatigue life. Ti64 alloy have always decreasing S-N curve at both RT and 400 °C. Fractrography demonstrated crack initiation sites at the surface for RT specimen and multiple crack initiation sites with fatigue steps at 400 °C. [1]

**G.Q. Wu** investigated the effect of microstructure on HCF properties of Ti64 alloys. For this he collected 75 sets of data from 21 reference that included HCF strength data and microstructure parameters of Ti64 alloy. All the fatigue tests were performed at room temperature under axial loading condition on unnotched hourglass specimen. According to the different fatigue life ($10^{5,}$ $10^6$, $10^7$cycles), the fatigue strengths of Ti64 alloys with three typical microstructures (bimodal, lamellar and equiaxed) were presented. The results showed that the HCF properties were strongly determined by microstructure types for Ti64. The S–N curves showed that the fatigue life increased as the loading decreased. The microstructure types of Ti64 alloy have significant influence on the HCF strength. Generally, the HCF strength of different microstructures decrease in the order of bimodal→lamellar→equiaxed microstructure. The α grain size in equiaxed microstructure or α lamellar width in lamellar microstructure has significant influence on the HCF strength. The HCF strength declines with the increasing of either α grain size or α lamellar width. Manufacturers can optimize the HCF

strength of bimodal microstructures by controlling the $\alpha_p$ volume fraction and αp size, respectively. The HCF strength can be controlled by a grain size or a lamellar width by volume fraction ranging from 30% to 50% and $\alpha_p$ size as small as possible. [2]

**K. Tokaji** worked on the effect of temperature (350 °C, 450 °C) on fatigue strength of the material and also, he correlated the crack initiation behaviour with respect to increase in temperature. Ti64 material was used followed by heat treatment. Result showed that the fatigue strength at elevated temperatures decreased significantly compared with that at ambient temperature. In the short life region, the fatigue strength was lower at 450 °C than 350 °C, while in the long-life region, it was nearly the same for both temperatures. The fatigue strength characterized in terms of the fatigue ratio also decreased at elevated temperatures compared with at ambient temperature. Crack initiation occurred relatively much earlier at elevated temperature, thus most of fatigue life was dominated by small crack growth. The small crack growth rates at elevated temperatures were considerably faster than those at ambient temperature, increasing with an increase in temperature. Fracture surfaces at elevated temperatures were rather brittle compared with those at ambient temperature and many secondary cracks were recognized on fracture surfaces, which were more noticeable with increasing temperature and applied stress. [3]

**R.J. Morrissey** work reflected on the effect of frequency at various stress ratio on HCF behaviour, this study is important for the design of gas turbine engines. Forged Ti64 bar were used followed by Vacuum Annealing heat treatment. Multiple heat treatment cycles were used to alter the microstructure characteristic of the material. Different stress ratios were used to test the material R = 0.1, 0.5, 0.8 at varying frequency 70, 400, 1800 Hz. Results indicated a frequency dependence that varies with stress ratio (*R*). At low *R*, the fatigue strength increases with increasing frequency. As *R* is increased, this trend continues until a transition zone is reached. Above this transition the frequency effect seems to vanish at the lower frequencies, but it is still apparent at high frequency [4]

### 2.1 Research gap

Most researchers have carried out high-temperature fatigue tests at 300 °C and above, but there is very little or almost no data available for tests done in the intermediate temperature range, like 150 °C. While research has mostly focused on very high frequencies, there is a lack of attention given to the material's own frequency or resonance frequency, which is around 77 Hz. No studies have been found that tested fatigue at 150 °C using a stress ratio of 0.5 and the material frequency of 77 Hz. Overall, investigations at 150 °C are quite limited. At this temperature, oxidation kinetics start affecting the surface properties, which can influence the points where cracks begin. There is also very little research on how vibrational stresses at resonance frequency interact with the formation of oxide layers and micro-cracks.

## 2.2 Fundamentals of Fatigue

### 2.2.1 High Cycle Fatigue (HCF)

As the name implies the number cycle is high, the material in which if the cycles run more than $10^5$ cycles of the applied load it is called HCF. So, the loads applied should be less than the yield strength. If the applied load is within the elastic limit the material can go far behind the $10^5$ cycles.

In HCF stresses and strains are largely confined to the elastic region. Low loads and long life. Applied stress is within the elastic range of the material and the number of cycles to failure is large. High-cycle fatigue is associated with life greater than 100,000 cycles.

### 2.2.2 Fatigue Limit

The stress level below which no fatigue failures occur is known as the fatigue limit. The fatigue limit, often referred to as the endurance limit, is the highest stress amplitude that a material can tolerate without undergoing fatigue failure, when subjected to a specified number of cycles. In other words, the fatigue limit is the stress level below which a material can undergo an infinite number of cycles of stress without failing due to fatigue.

### 2.2.3 S-N curve

A statistical illustration of material fatigue behaviour under cyclic stress circumstances is the SN Curve. To ascertain the fatigue strength and endurance limit of materials under repeated loading circumstances, High Cycle Fatigue (HCF) testing is frequently performed. For HCF, the Stress-Life (S-N) model is frequently utilised. It is one method for determining a material's fatigue life, and its main focus is on fatigue failures at high cycle counts ($N>10^5$). A graph of applied stress (S) and failure cycles (N) is displayed. The limit, where the S-N curve becomes flat at larger N values, is only present in a small number of ferrous (iron-base) and titanium alloys. Aluminium and copper, two structural metals, do not have any set limits. The SN curve is used in HCF testing to forecast a material's fatigue life under repeated loading scenarios. For a range of stress amplitudes, it is to forecast the number of cycles till failure. It is possible to determine the fatigue strength that corresponds to its cycle count. It makes it simple to determine the material's endurance limit.[5]

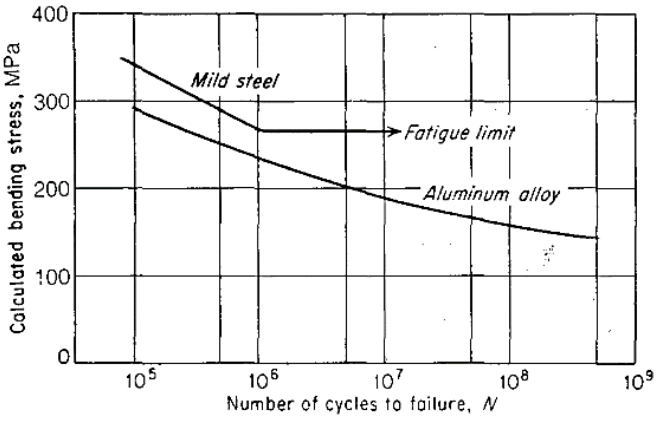


Figure 2.1. Fatigue S-N curves [5]

### 2.2.4 Fatigue test parameters

During a load cycle, the stress changes between a maximum stress $\sigma_{max}$ and a minimum stress $\sigma_{min}$. The stress amplitude is represented by $\sigma_a$ and the mean stress is represented by $\sigma_m$

Stress ratio is represented by R.

R = $\sigma_{min}/\sigma_{max}$ .....equation 1

Mean stress, $\sigma_m = (\sigma_{max} + \sigma_{min})/2$ ……equation 2

Stress amplitude, $\sigma_a = (\sigma_{max} - \sigma_{min})/2$ ……equation 3

## 2.2.5 Types of cyclic loading

The types of cyclic loading that can lead to fatigue failure in materials are shown in fig 2.2. In repeated stress, the material is subjected to a cycle of loading and unloading in the same direction in reversed stress, the material is subjected to a cycle of equal magnitude and opposite direction. A type of cyclic loading known as variable cyclic loading involves changing the applied load over time. This may incorporate variations in the mean stress as well as combinations of high and low stress amplitudes.

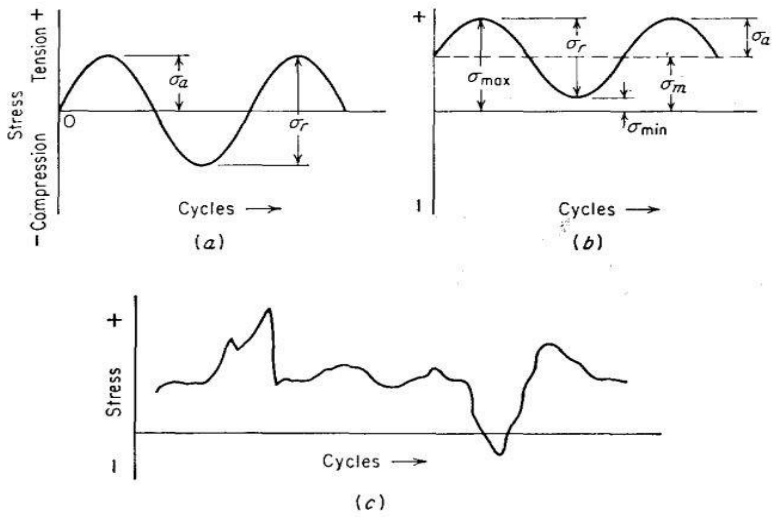


Figure 2.2. Types of stress cycles in fatigue load a) Reversed stress b) Repeated stress c) Random stress [5]

## 2.2.6 (a) Variable loading

Instead of keeping load constant for the entire cycle, the load is kept on changing. Without applying the full load up to its failure, the load is applied gradually changes through several of steps. The constant amplitude of the R- Ratio keeps on changing or the parameter can be kept constant for certain time period.

Variable loading can take many forms, including random loading, spectrum loading, and block loading. Random loading refers to loading conditions where the amplitude and frequency of the load vary randomly over time. Spectrum loading refers to loading conditions where the amplitude and frequency of the load are known and follow a specified distribution. Block loading refers to loading conditions where the load alternates between two or more constant amplitudes for a specified number of cycles.

Variable loading can significantly affect the fatigue behaviour of materials and structures. Under variable loading conditions, the material experiences varying levels of stress, and the number of cycles to failure may be reduced compared to constant amplitude loading. The type of variable loading also affects the material's fatigue behaviour. For example, block loading can lead to crack initiation and propagation, while spectrum loading can lead to material degradation due to plastic deformation.

To evaluate the fatigue behaviour of materials under variable loading conditions, specialized testing methods and equipment are required. Variable amplitude fatigue testing machines are used to simulate real-world loading conditions and to determine the material's fatigue life under variable loading. These machines are capable of applying loads with varying amplitudes and frequencies, and can also simulate different loading conditions, such as random, spectrum, and block loading.

The results of variable loading fatigue tests are important for designing components and structures that are less prone to failure under variable loading conditions. By understanding the fatigue behaviour of materials under variable loading, engineers can design components that are more durable and can withstand a wider range of loading conditions.

### 2.2.7 (b) Block loading

Block loading is a type of variable loading. Block loading refers to loading conditions where the load alternates between two or more constant amplitudes for a specified number of cycles. Here, 10 blocks of amplitude stress is applied on the alloy. The loading sequence is from low to high. With a mean stress of 66 MPa, the stress amplitude load from 260 MPa to 305 MPa have been applied with a step size 5 MPa. Each block of the block loading has a specified number of cycles. So, it has $10^7$ cycles of each 10 blocks in a sequence maintaining the constant mean load over the entire test explained in fig 2.3.

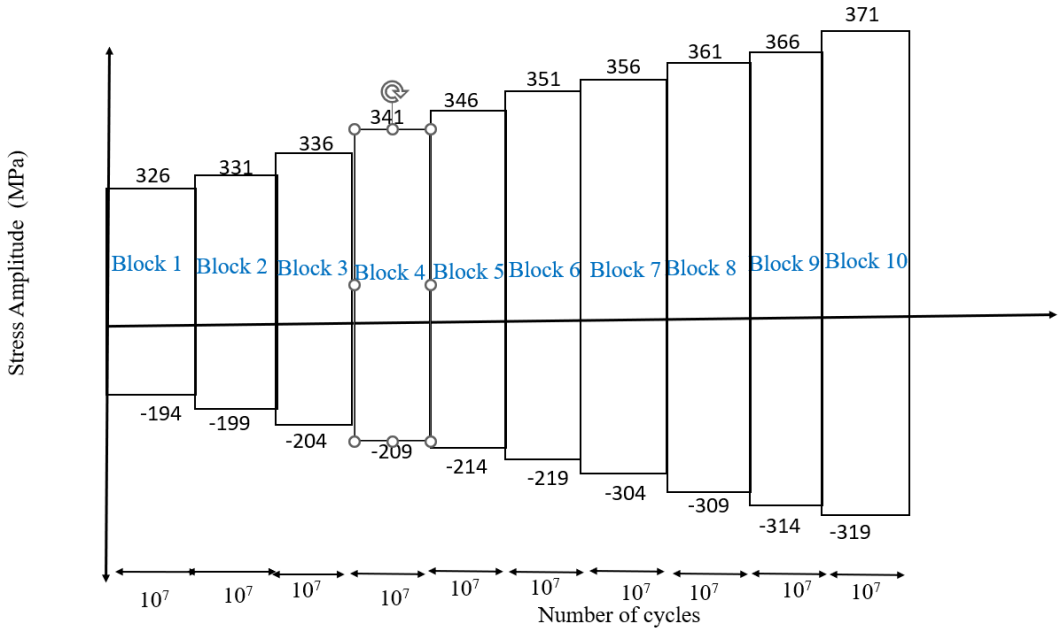


Figure 2.3. Applied block loads

## 2.3 Fracture

The splitting or cleavage of a solid body into multiple fragments as a consequence of stress is known as fracture. It is possible to divide the fracture mechanism into three parts:

(i) Crack initiation

(ii) Crack propagation

(iii) Final fracture

### (i) Crack Initiation

The crack initiation can occur because of the inclusion present or from the notches or even in a defect free surface by crack roughening. The dislocation under the cyclic load can roughen the surface generates the crack, where a little fracture develops at a location with a high stress concentration. Under cyclic stresses, cracks begin as the component's surface becomes rougher due to plastic deformation. Dislocation movement on slip planes can create intrusions and extrusions, which can roughen a surface. Steps that were created on the surface by the material's slip are not entirely erased. Following load reversal because a dislocation that has shifted in one direction won't always go back to where it was. Instead, another dislocation may shift and bring about the plastic deformation, causing the initially smooth

surface to become rough. This can be seen by the movement of slip as a slip band in the form of extrusion and intrusions as shown in fig 2.4.

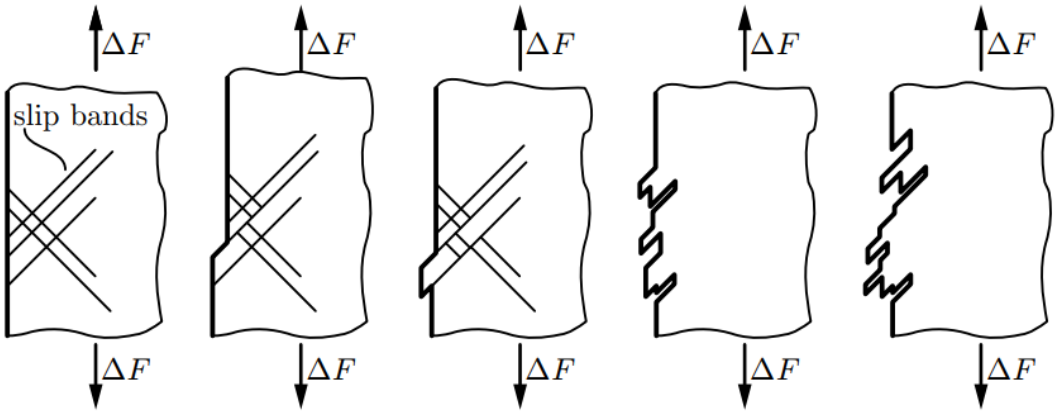


Figure 2.4. Formation of slip bands as extrusions and intrusions

## (ii) Crack Propagation

Stage 1: They prefer to grow in grains with slip planes that are oriented roughly 45 degrees away from the primary stress maximum. It propagates by the mode 2 and 3 (based on the stress interaction with crack, 2 The forward shear mode, describes a shear stress that is applied normal to the crack's leading edge but in its plane, 3- The corresponding shear mode is for shearing forces that are applied parallel to the crack's leading edge).

Stage 2: The stage 1 crack after reaching the grain boundary, the crack gets stopped as the crack boundary acts as a barrier as there is no slip planes to move further. Initial cracks cease to expand, and only those that unintentionally begin to do so under ideal circumstances do so.The stress at the fracture tip increases with increased crack propagation to the point where less well-oriented slide systems can become active. As a result, the crack might alter its orientation to mode 1, which is perpendicular to the primary stress that is highest. The crack expands into a macro crack.

## (iii) Final Fracture

Fractures is subdivided into two broad groups:

## (a) Ductile fracture

When a material has extensive plastic deformation prior to failing, it might experience a material failure known as a ductile fracture shown in fig 2.5. Metals, alloys, some polymers, and this type of fracture are frequently seen in these materials. A ductile material will start to deform plastically, or permanently deform without breaking, when stress or strain are applied to it that exceeds its elastic limit. The material will eventually reach a point during the deformation where it can no longer withstand the imposed stress and will fracture. Significant deformation and warning signals, such as necking or localised material thinning, frequently precede ductile fracture. Tensile, compressive, and shear loading are only a few of the different loading scenarios that can result in ductile fracture. A ductile material's fracture surface typically has a fibrous look and is marked by visible deformation bands or markings that show the direction of plastic deformation.

The most typical type of ductile fracture is called a cup-and-cone fracture because it has a conical protrusion on one side and a cup-shaped depression on the other of the fracture surface. Shearing of the material under considerable plastic deformation causes the cup and cone pattern.

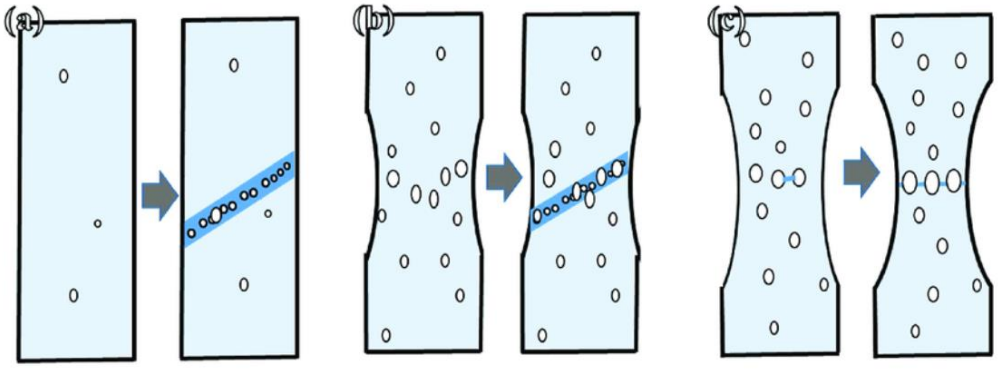

Figure 2.5 a) Failure by localised plastic without necking b) Failure by localised plastic with necking c) Failure by void coalescence with obvious necking [4]

## (b) Brittle fracture

When a material breaks quickly and without warning under a relatively small amount of stress or strain, it is said to have had a brittle fracture. At low temperatures, this kind of fracture is frequently seen in brittle materials like ceramics, glasses, and some metals. Brittle fracture happens with little to no plastic distortion, in contrast to ductile fracture, which

requires significant plastic deformation before fracture. This is due to the limited ductility of brittle materials and their inability to undergo significant plastic deformation prior to fracture.

Rapid crack propagation through the material is a sign of brittle fracture, which is distinguished by little to no apparent deformation before the fracture. A brittle material's fracture surface will typically be smooth and flat, indicating that the fracture was caused by the spread of a single crack. High stress concentrations, the presence of flaws or imperfections in the material, and exposure to low temperatures are only a few causes that can lead to brittle fracture. Brittle fracture can occasionally be avoided by lowering stress concentrations, managing the size and distribution of flaws, and improving the material's ductility through alloying or heat treatment. Brittle fractures come in a variety of forms that can be categorised according to how they spread or how they appear on the fracture surface.
Transgranular fractureis a kind of brittle fracture happens when a crack develops within a material's grains as opposed to a long grain boundary. Transgranular fractures frequently have a conchoidal, flat, or smooth surface.Intergranular fracture is a break in a material that spreads along the borders between grains. Transgranular fractures often have a smoother surface than intergranular fractures, although intergranular fractures may have noticeable steps or ridges along the fracture surface [5].

Cleavage fracture is a type of brittle fracture occurs when a crack propagates along a specific crystallographic plane within a material, resulting in a flat, smooth fracture surface. Usually, "river marking" can be seen on the flat facets. The break in the crystal, which travels over several parallel planes to produce a succession of plateaus and connecting ledges, is what creates the river patterns. These are signs that localised deformation has absorbed energy. The "river patterns"' direction corresponds to the crack's propagation direction.Among the frequent varieties of brittle fracture are shown in fig 2.6.

## 2.4 Failure Modes

In fracture mechanics, three distinct load scenarios are distinguished based on how the stresses interacts with the crack. They are referred to as Mode 1 to 3 as shown in fig 2.6. Mode 1- the biggest primary stress in stage I is aligned perpendicular to the crack surface.A

tensile stress applied in the direction normal to the fracture faces is known as mode 1, the crack-opening mode.

Mode 2-The forward shear mode, describes a shear stress that is applied normal to the crack's leading edge but in its plane.

Mode 3- The corresponding shear mode is for shearing forces that are applied parallel to the crack's leading edge.[6].

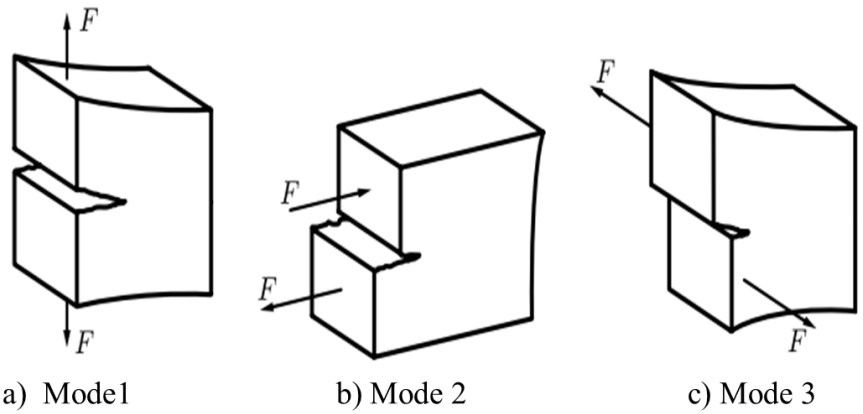


Figure 2.6. Modes of crack formation [8]

## 2.5 Fatigue Failure

The damage of a material due to cyclic loading much below its tensile strength or yield strength is called fatigue. Compared to a single applied load the material whose load cyclically varies from tension to compression repeatedly fails after undergoing a lot number of cycles. When the stress is more than the number of cycles required for the material to break is less, and when the stress is less the number of cycles required for it to break is more. Because it happens suddenly and without any clear warning, a fatigue failure is dangerous. Usually, a fracture surface's appearance can be used to identify a fatigue failure because of the rubbing motion that spread throughout the area, the surface is smooth. A component with a rough area failed ductility. A succession of rings for beach marks typically shows the fracture's progression. The fatigue fractured surface is rough, while the initiation and the propagation part of the fracture is smooth surface.

The fatigue process has three stages of damage evolution

1 Crack initiation.

2 Crack propagation, and

3 Catastrophic failures

Three fundamental causes can result in fatigue failure.

1. The greatest tensile stress
2. Variation in the stress applied
3. A significant number of stress cycle

# Chapter 3

# EXPERIMENTAL DETAILS

Based on the research gap experimental methodology was designed. This chapter covers methodology followed, materials used, instruments used.

## 3.1 Material: Ti64 alloy

The Alloy Ti64 is a Titanium based (α+β) alloy with composition of as received samples as shown in the Table 3.1, as per MiDhaNi designation TITAN 31A

Table 3.1. Chemical composition of Ti64 alloy

| **Elements** | **Chemical composition (wt %)** |
|---|---|
| Ti | Bal |
| Al | 6.46 |
| V | 4.09 |
| O | 0.18 |
| Fe | < 0.10 |
| Mo | 0.1 |
| C | 0.02 |
| N | 0.0095 |
| H | 0.0045 |
| Sn | < 0.01 |
| Cu | 0.002 |
| Mn | 0.002 |
| Zr | < 0.1 |

## 3.2 Specimen Details

High cycle fatigue tests were performed on standard fatigue specimens which were machined according to the ASTM E466-15 standard. The specimen used is of total length of 91 mm and diameter of 6 mm as shown in figure 3.1.

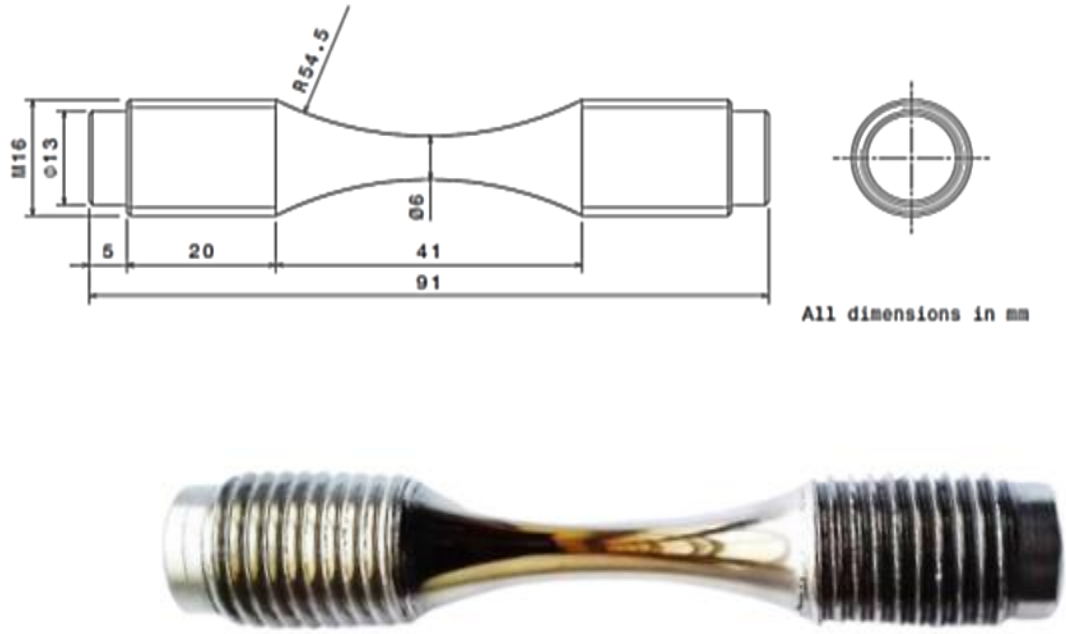


Figure 3.1. Geometric drawing and picture of High cycle fatigue hour glass specimen as per ASTM E 466

## 3.3 Test Matrix

The test matrix were designed based on yield strength of the material, at incremental stress of 50 MPa.

Table 3.2: Test Matrix of Ti64 Alloy

| | RT & 150 °C | | | | | | |
|---|---|---|---|---|---|---|---|
| **Maximum Stress (MPa)** | 600 | 700 | 750 | 800 | 850 | 900 | 950 |

## 3.4 Methodology adopted

- Sample was prepared according to the ASTM E 466 standard. Uniform gauge length of 41 mm and diameter of 6 mm with length to diameter ratio 7.3 is used
- Test matrix was prepared and according to it, fatigue tests were performed on RUMUL 100 kN resonance fatigue testing machine at RT and 150 °C. Test stop criterion was $10^7$ Cycles. SN curves were generated
- After the run out or failure of the specimen, samples were cut for further analysis

- Characterization of microstructure was done on optical metallurgical microscope and on Scanning Electron Microscope (SEM)
- Fractography of failed fractured specimen was done using SEM in order to determine the mode of failure
- Hardness was found out by using Vickers micro hardness tester

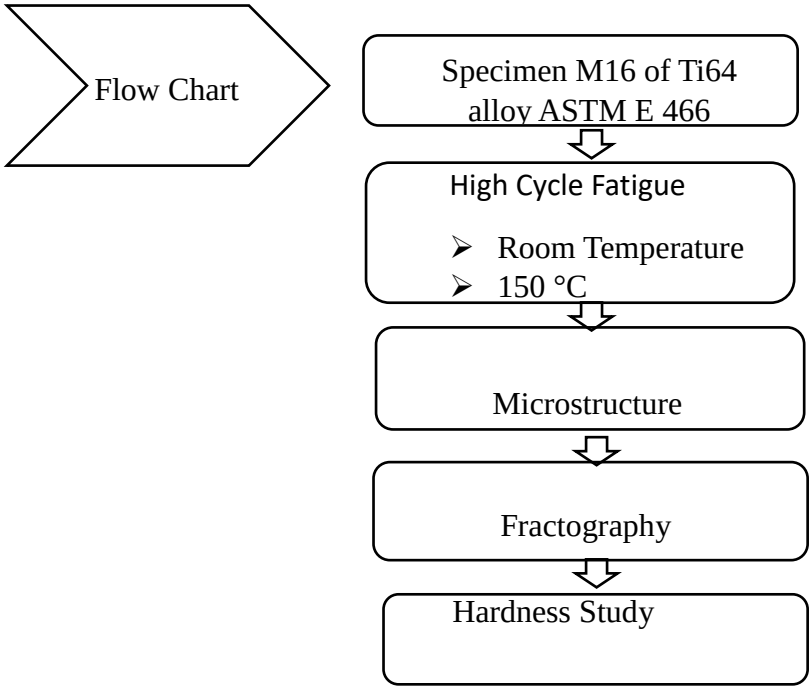


Figure 3.2: Experimental Flow Chart Analysis details of fatigue tested specimen

## 3.5 Equipments Used

### 3.5.1 Rumul testing machine

RUMUL HCF (High Cycle Fatigue) testing machine, shown in figure 3.3, is a type of fatigue testing machine used to evaluate the fatigue strength of materials subjected to high-frequency loading conditions. It is typically used for testing metallic materials such as steel, aluminium, and titanium alloys that are commonly used in aerospace, automotive, and other high-performance applications. The RUMUL HCF testing machine is designed to apply cyclic loads at frequencies ranging from 20 Hz to 250 Hz, with a maximum load capacity of 100 kN. The machine is equipped with a high-speed hydraulic actuator that allows for precise control of the loading frequency and amplitude. It also has an automatic specimen alignment system that ensures accurate and repeatable testing results. During testing, the specimen is clamped between two grips and subjected to cyclic loading at a predetermined frequency and

amplitude. The loading cycle is typically sinusoidal in shape and the amplitude is usually set to a percentage of the material's ultimate strength. The number of cycles to failure is recorded and used to calculate the material's fatigue strength. The RUMUL HCF testing machine can be used to evaluate the fatigue strength of materials under a range of loading conditions. It is also capable of performing tests at moderately elevated temperatures to simulate real-world operating conditions. The testing data obtained from RUMUL HCF testing machine is useful for predicting the fatigue life of materials in real-world applications and also for designing components that are less prone to failure due to fatigue

A resonator-based, oscillating system operates at its natural frequency to produce the dynamic load. The machine is separated into a static and dynamic part and allows to perform dynamic test at any selected stress ratio. Here, both alternating and mean stresses are under control. The alternating stress is controlled by the dynamic drive. The mean stress is controlled by the static load drive. This machine has a maximum load capacity of 100 kN. The specimen is mounted between the pull rod cylinder assemblies (top and bottom) and the stress values are applied.

Figure 3.3. RUMUL High Cycle Fatigue (HCF) testing machine

### 3.5.2 Testing methodology

Constant amplitude fatigue tests were conducted for stress ratio (R) = 0.5 at RT and 150°C.The run out test stop ratio was $10^7$ cycles. The stress level at which test was conducted at each temperature are shown table 3.2. Microstructure, Fractrographic and hardness studies were carried out on samples failed due to fatigue. Owing to the stiffness and density of the material being tested, the frequency attained during the test was 77 Hz. So, for the completion of one runout test of $10^7$ cycles it takes approximately 2 days.

### 3.5.3 EDM machine

EDM stands for Electro-Discharge Machining. Here, electrical energy is used to erode or remove material from a workpiece. It is a non-traditional machining technique. In EDM machine shown in figure 3.4, a spark is produced between the electrode and the workpiece using a thin wire or electrode. The material is melted and vaporised by the spark's tremendous heat, which is subsequently washed away by a dielectric fluid.

Figure 3.4. Electro discharge machine (EDM)

### 3.5.4 Hot mounting machine

A device called a hot mounting machine shown in figure 3.5, is used to prepare samples for microscopic examination. For sectioning and polishing, it is used to insert tiny or a typically shaped metal samples into a resin or plastic substrate. The metal sample is put into a mould that has plastic or a thermosetting resin inside of it as part of the hot mounting procedure. The mould is then put into a hot mounting machine, which uses pressure and heat to solidify the resin and form a solid block around the sample. The sample is properly lodged in the resin and is free of any voids or air pockets that can interfere with the future sectioning and polishing procedures.

Figure 3.5. Hot mounting machine

### 3.5.5 Polishing machine

For the preparation of metallographic samples, material science laboratories employ the disc polishing machine. Hard materials including ceramics, composites, and hardened steels can be polished and finished using this machine.

The disc polishing equipment from Bainpol Metco (figure 3.6) has a durable design and accurate polishing capabilities. The apparatus has a big polishing disc that can accommodate multiple samples at once and a variable-speed motor that enables the user to control the polishing pace.

In order to keep the sample and polishing disc from overheating and distorting during the polishing process, the machine is fitted with a water-cooling system.

The disc polishing machine is frequently used to prepare metallographic samples for microscopic examination. Optical or scanning electron microscopy can be used to analyse the polished samples in order to determine their microstructure and content.

The "grade" of a particular type of abrasive paper refers to the size or coarseness of the abrasive particles. In order to remove material or shape a surface, abrasive materials are employed in a variety of applications like sanding, grinding, and polishing.

When deciding which paper is best suitable for a certain application, the abrasive paper's grade is a crucial factor to take into account. The size of the abrasive particles determines the grade, which is frequently represented by a number. Lower the number, the abrasive particles

will be coarser and able to remove more material. In contrast, a higher number denotes a smoother finish and smaller abrasive particle size.

The grade paper used were of 600,800,1000,1200,1500 and 2000 grits one after other respectively.

Figure 3.6. Polishing machine

### 3.5.6 Etching

Etching is a technique used to expose a material's surface microstructure. In order to reveal the material's microstructure, the material's surface need to be carefully polished and etched using proper emery papers and etchant.

When surfaces are etched with an etchant, it is used to increase the contrast so that the microstructure is seen with the microscope. Chemical etching may enable detection of microstructure. The etchant used for this sample is Krolls reagant (3 ml HF + 6 ml $HNO_3$ + 91 ml $H_2O$) and approximately (5 -10) seconds required to etch the specimen.

### 3.5.7 Optical microscope

The optical microscope is used to study the properties and behaviour by revealing materials microstructure. It uses reflection of light for illumination. Metallurgical Microscope has two distinct optical systems, namely, Objective and Eyepiece. Combination of both of these will render the magnified virtual image of the same under observation. For effective handling of

the Microscope, it is essential that the Metallurgists should know the working principle of the microscope and fundamental terminology related with basic optical systems.

An optical microscope works under the principle that a beam of light from appropriate source is incident on to the surface of specimen through the objective. A certain amount of this incident light reflected from the specimen surface and magnified while passing through the objective and the eyepiece and will form enlarged image of the illuminated area.

A non-destructive method for observing and examining the microstructure of materials is optical microscopy shown in figure 3.7. Using optical microscopy, optical micrography is the process of taking and examining pictures of the microstructure of materials.

Figure 3.7. Optical metallurgical microscope

### 3.5.8 Scanning electron microscopy (SEM)

SEM analysis stands for Scanning Electron Microscopy analysis shown in figure 3.8. It is a powerful analytical technique used in materials science and engineering to investigate the microstructure and surface topography of materials.

In SEM analysis, a beam of electrons is focused on the surface of a sample, causing the emission of secondary electrons and backscattered electrons from the surface. These electrons are collected and used to form an image of the sample's surface, providing detailed information about the material's microstructure, composition, and topography. SEM model used for this study was Jeol JSM 6380A

Figure 3.8. Scanning electron microscope (SEM)

### 3.5.9 Micro Vickers Hardness

The machine used to test the Vickers micro hardness is Mitutoyo HM-200, shown in figure 3.9. Vickers micro hardness testing is a kind of hardness assessment that analyses a material's resistance to being indented by a diamond indenter.

Figure 3.9. Vickers micro hardness testing machine

A digital microscope on the HM 200 AVPAK 20 (software) allows for accurate measurement of the indentation and precise positioning of the diamond indenter. The microscope is connected to the computer, which manages the test parameters and records the test outcomes. The sample is subjected to a 300-gram force

# Chapter 4

## RESULTS AND DISCUSSION

The experimental results obtained from fatigue testing, optical microscopy, scanning electron microscopy, fractrography, micro hardness are presented and discussed in this chapter

Table 4.1: Fatigue test results of Ti64 alloy

| **Maximum stress ($\sigma_{max}$, MPa)** | **Cycles** | |
|---|---|---|
| | **RT (Nf)** | **150 °C (Nf)** |
| 950 | 162725 | 35730 |
| 900 | 1833061 | 140980 |
| 850 | 5526041 | 958450 |
| 800 | 8246806 | 4611990 |
| 750 | $10^7$ | 9894460 |
| 700 | $10^7$ | $10^7$ |
| 600 | $10^7$ | $10^7$ |

Results from HCF tests conducted for RT and 150 °C are shown in the table 4.1. It is observed that the fatigue life is found to reduce with increase in maximum stress. RT results indicate that the specimens went for runout up to 750 MPa and the life started decreasing from 850 MPa. 150 °C tests show that specimens went for runout up to 700 MPa and the life started decreasing after that.

## 4.1 S-N Curve

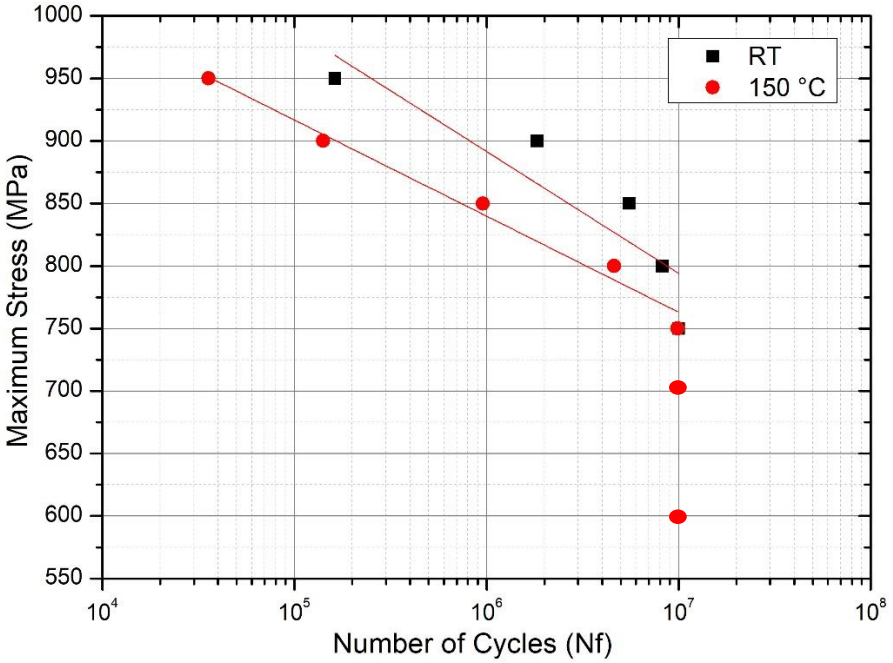


Figure 4.1: S-N Curve for Ti64 alloy

The S-N Curve also known as Stress Life Curve, is a graphical representation of the relationship between the maximum stress (S) applied to a material and the number of cycles to failure (N). It is a fundamental tool in fatigue analysis, used to predict the lifespan of materials under repeated loading-Axis represents the Number of cycles to failure (N), typically range from below$10^5$ cycles (Low cycle fatigue) and above $10^5$ cycles (High Cycle fatigue). Y- Axis represents the maximum stress (S) applied in each cycle.

At higher stress level 900 MPa a drop in fatigue life was observed by 92% as compared to room temperature, whereas at lower stress level there is not much effect of the temperature.

A maximum percentage decrease in life of 92.31 from RT to 150 °C is observed at a maximum stress level of 900 MPa.

The endurance for Room temperature was 750 MPa while endurance for 150 °C is 700 MPa

At lower stress level drop in life is not much and for 750 MPa drop in life was 2 percent.

In SN curve the effect of temperature is found to be reduced with increase in number of cycles. Slopes of 150 $^oC$ is found to be more as compared to RT. With increase in maximum stress the effect of temperature on number of cycles is more.

## 4.2 Microstructure

### 4.2.1 Optical Microscopy

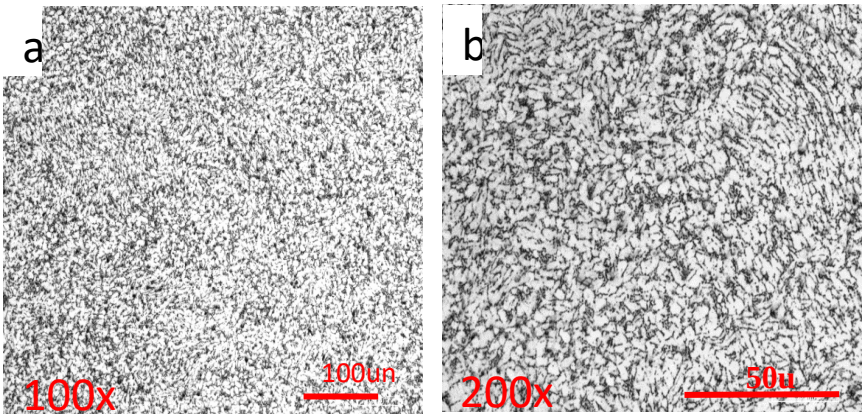


Figure 4.2: A as-received Ti64 alloy showing optical microstructure (a, b,) at 100x, 200x,)

The optical micrographs of a Ti64 samples were taken at a magnification of 100x and 200x and the same is shown in the figure 4.2. In optical micrographs it has been seen that, the equiaxed grains are at various magnification. Alpha (α) light region and beta (β) dark region were seen on the structure. The α percentage covers 60% of the region while the rest is covered by the β grains when observed under 100x magnification. The alpha phase is stabilised by the Al, O, N, C, while the beta phase is stabilized by V and Mo.

### 4.2.2 Scanning Electron Microscopy

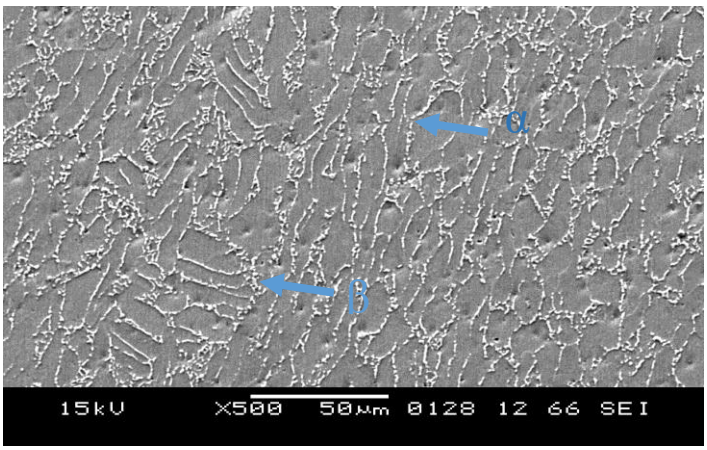


Figure 4.3: SEM structures showing the in-depth morphology of as received specimen

The SEM (Scanning Electron Microscope) microstructure of Ti-6Al-4V alloy typically reveals several key features. Alpha (α) phase appears light, needle or plate like structures. This is primary hexagonal close-packed (HCP) phase, providing strength and good fatigue resistance. Beta (β) phase darker regions compared to α-phase, with a more equiaxed or transformed appearance. Body centered cubic (BCC) structure, contributing to ductility and workability, usually observed at grain boundaries or with α colonies after heat treatment.

The Ti64 alloy consists of 6% Aluminium (Al) and 4% Vanadium (V) with the balance being Titanium (Ti).Aluminium stabilizes the- phase, while Vanadium stabilizes the β-phase.Semi-equiaxed or equiaxed microstructure is characterized by a mix of equiaxed α grains in a more elongated form. This can be achieved through specific heat treatment or thermomechanical processing that promotes partial recrystallization.

### 4.2.3 Optical Microscopy

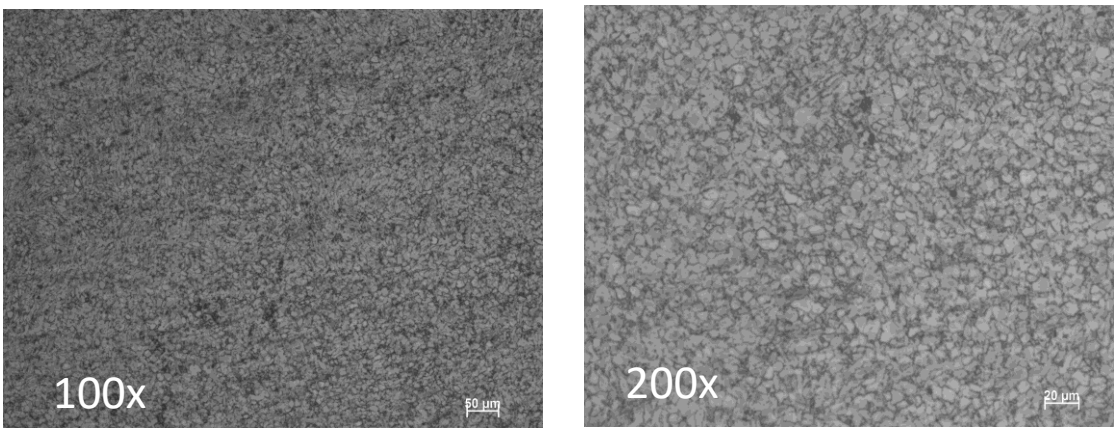


Figure 4.4 Microstructure of cyclically failed specimen

The optical microstructure of a Ti64 fatigue tested failed specimen at 100x magnification is shown in figure (4.4). The (α+β) phase becomes finer due to dynamic strain ageing. The α-phase grains may exhibit elongated or distorted shapes due to cyclic loading, while the β-phase regions may show evidence of localized stress. In region of high stress, α/β interfaces can become areas of crack deflection or secondary cracking.

## 4.3 Fractrography

**A) Analysis of Failed Ti64 alloy showing Fractrograph of Room Temperature (RT) tested specimen**

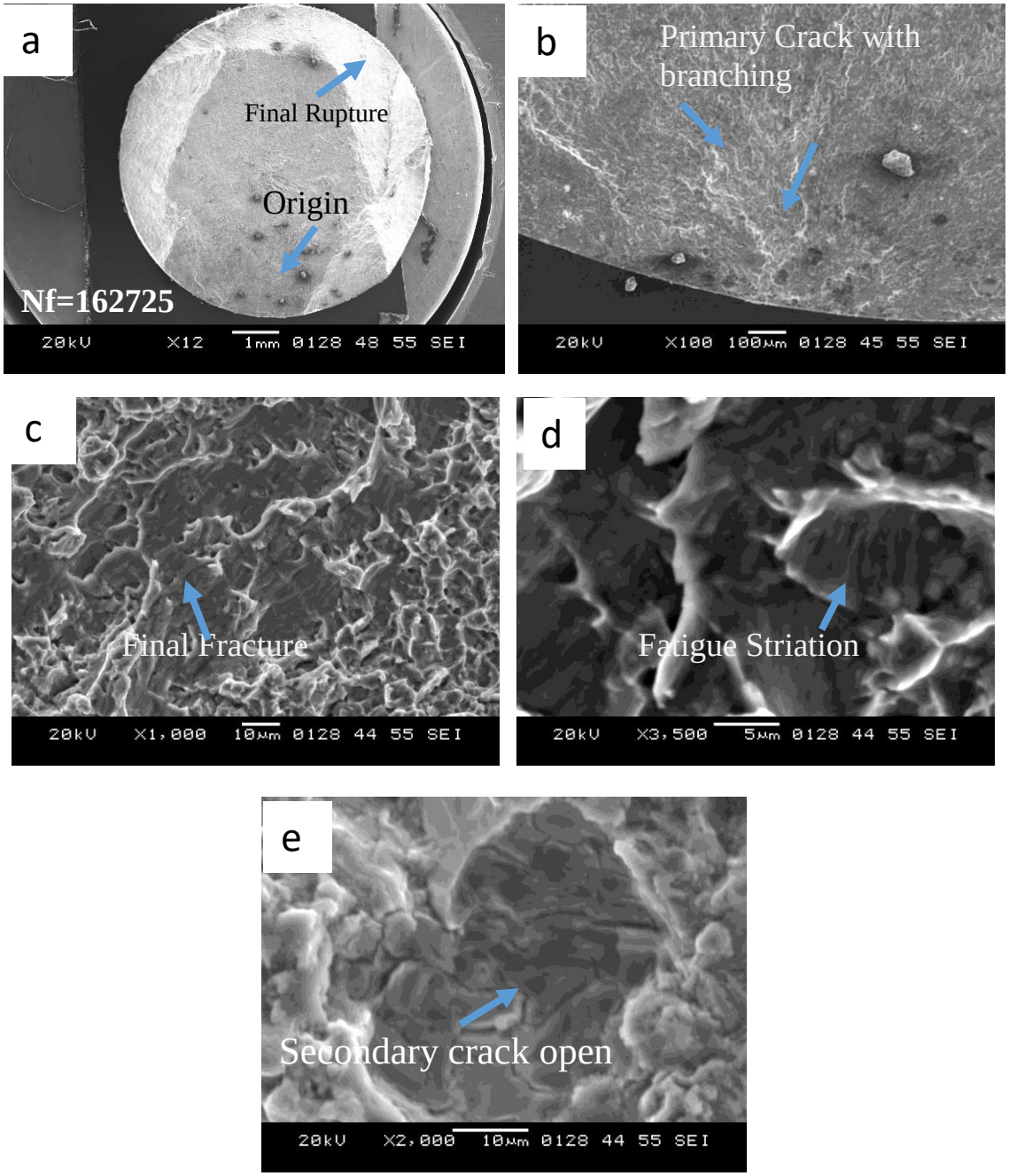


Figure 4.5.A: SEM Fractrograph showing the in-depth morphology of the fracture (a-e) RT 750 MPa, Fig (a, b) showing overall fracture surface & crack initiation sites, (b) showing the enlarged view of crack propagation,(c,d,e) showing the final fracture region with various features.

**B) Analysis of Failed Ti64 alloy showing Fractrograph of moderately elevated temperature (150°C) tested specimen**

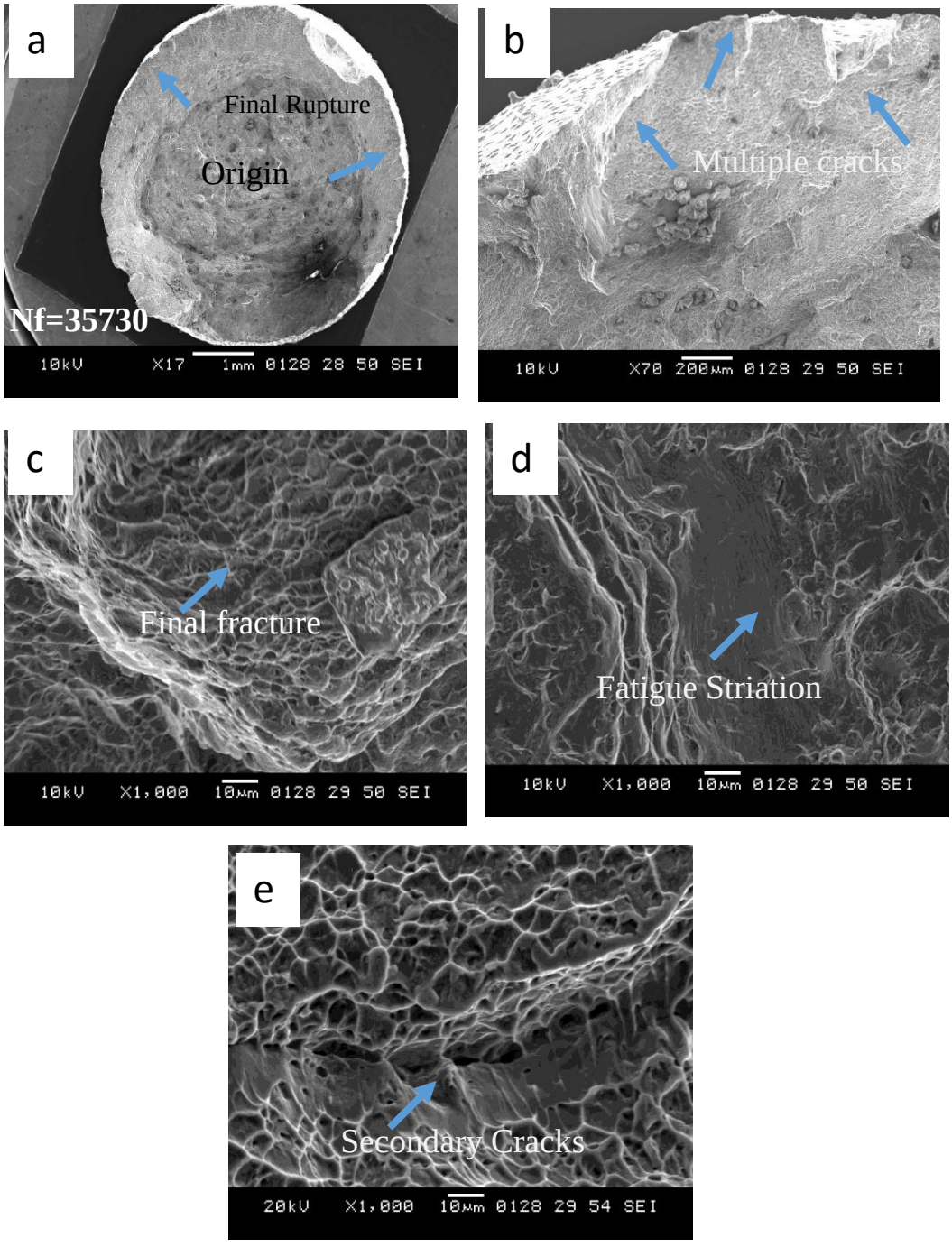


Figure 4.5.B: SEM Fractrograph showing the in-depth morphology of the fracture (a-e) 150 °C - 750 MPa &Fig (a & b) showing overall fracture surface & crack initiation sites, (b) showing the enlarged view of crack propagation, Fig (c, d, e) showing the final fracture region with various feature.

The fractrography of a failed Ti64 specimen under Scanning Electron Microscope (SEM) reveals characteristic features based on the failure mechanism.

Ductile Brittle Fracture were observed for RT specimen figure 4.5.A. On final fracture site ductile fracture were observed and it characterized by round, deep dimple indicating micro-void coalescence. The origin of the crack surface shows brittle fracture which appears as flat, shiny, reflective surfaces with distinct patterns. The crack initiation and propagation site were clearly observed on the sample surface.

Ductile fracture was observed for 150°C tested specimen in figure 4.5.B. Fully ductile fracture was observed when we enlarged the final fracture surface. Dimples were observed, these are formed by micro void coalescence. Multiple crack initiating sites were observed. Fatigue striation and secondary cracking coalescence were observed.

When a Ti64 specimen fails, the fractography observed under Scanning Electron Microscope (SEM) provides critical insights into the failure mechanism.

In case of ductile fracture, the fracture surface is dominated by numerous dimples, indicating micro-void coalescence. The dimples are typically formed around inclusions or second-phase particles and a hallmark of significant plastic deformation before final separation.

The presence of shear lips around the edges may also be visible, suggesting localized shear during the final stage of failure.in contrast, if the specimen undergoes brittle fracture, the SEM image reveals cleavages facets, smooth, flat surfaces indicative of crack propagation along crystallographic planes with minimal plastic deformation.

Additionally, river patterns and chevron marks may be present, pointing towards the origin of cracks initiation and its propagation path. In some cases, intergranular cracking was observed, where the fracture propagates along grain boundaries, often linked to environmental factors or heat treatment anomalies.

Occasionally, a mixed-mode fracture is identified, combining both ductile dimpling and brittle facets, particularly in fatigue or stress-corrosion environments.

The distinct SEM features of ductile and brittle fractures help in diagnosing the failure mode and understanding the materials response to applied stresses.

## 4.4 Energy Dispersive Spectroscopy (EDS) analysis

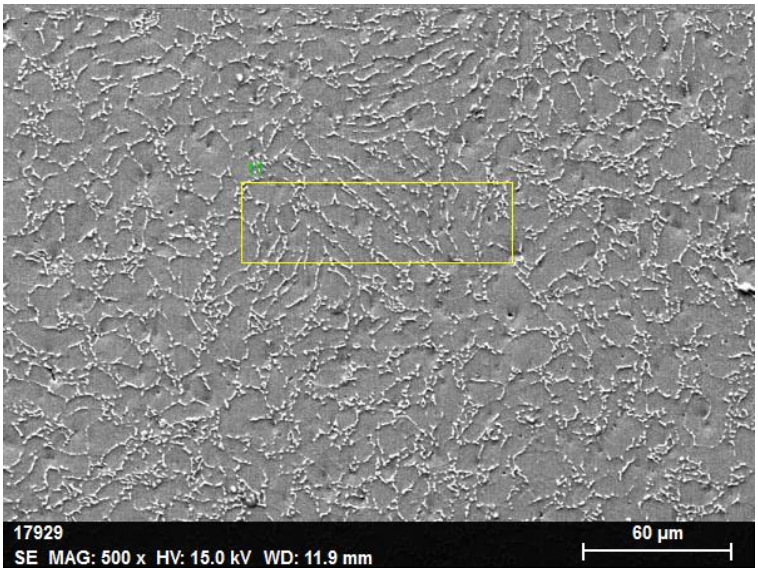


Figure 4.6: SEM structure showing EDS mapped region

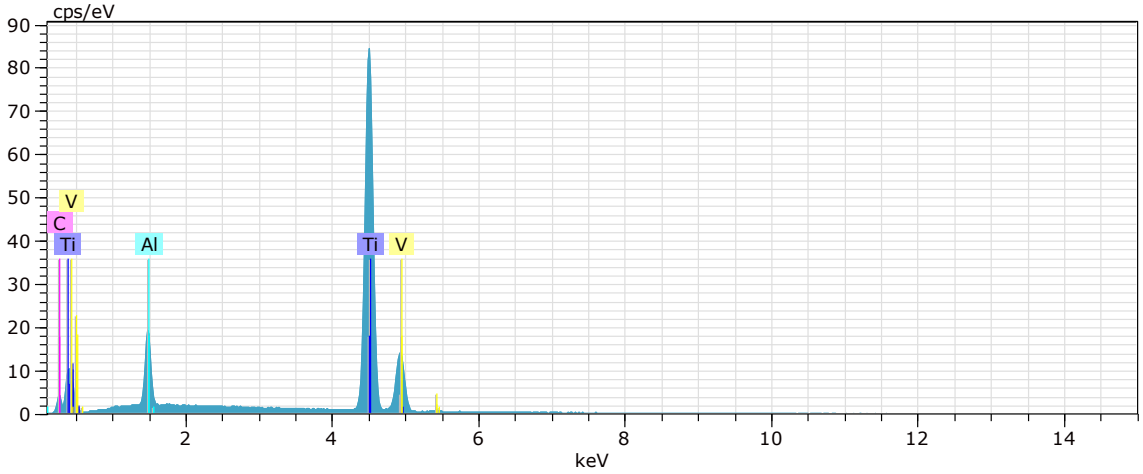


Figure 4.7: EDS graph showing elemental peak

| El | AN | Series | unn. C [wt.%] | norm. C [wt.%] | Atom. C [at.%] | Error (1 Sigma) [wt.%] |
|---|---|---|---|---|---|---|
| Ti | 22 | K-series | 88.10 | 86.95 | 74.01 | 2.57 |
| Al | 13 | K-series | 5.51 | 5.44 | 8.21 | 0.28 |
| C | 6 | K-series | 4.57 | 4.51 | 15.29 | 0.75 |
| V | 23 | K-series | 3.14 | 3.10 | 2.48 | 0.12 |
| | | Total: | 101.32 | 100.00 | 100.00 | |

Energy Dispersive Spectroscopy (EDS) analysis provides elemental composition information of a material. It is commonly used in conjunction with Scanning Electron Microscopy (SEM).

The EDS marked region in figure 4.7 confirm the titanium, aluminium and vanadium are present in the material.

Element Identification: Each peak in EDS spectrum corresponds to a specific element based on its characteristic X-ray energy.

Relative Elemental Composition: The height or intensity of each peak indicates the relative amount of that element present in the scanned area.

Qualitative Analysis: Confirms which element are present in the material (Ti, Al, V in TI64)

Semi-Quantitative Analysis: Provides approximate weight (%) and atomic (%) concentration of each detected element.

## 4.4 Vickers Micro Hardness

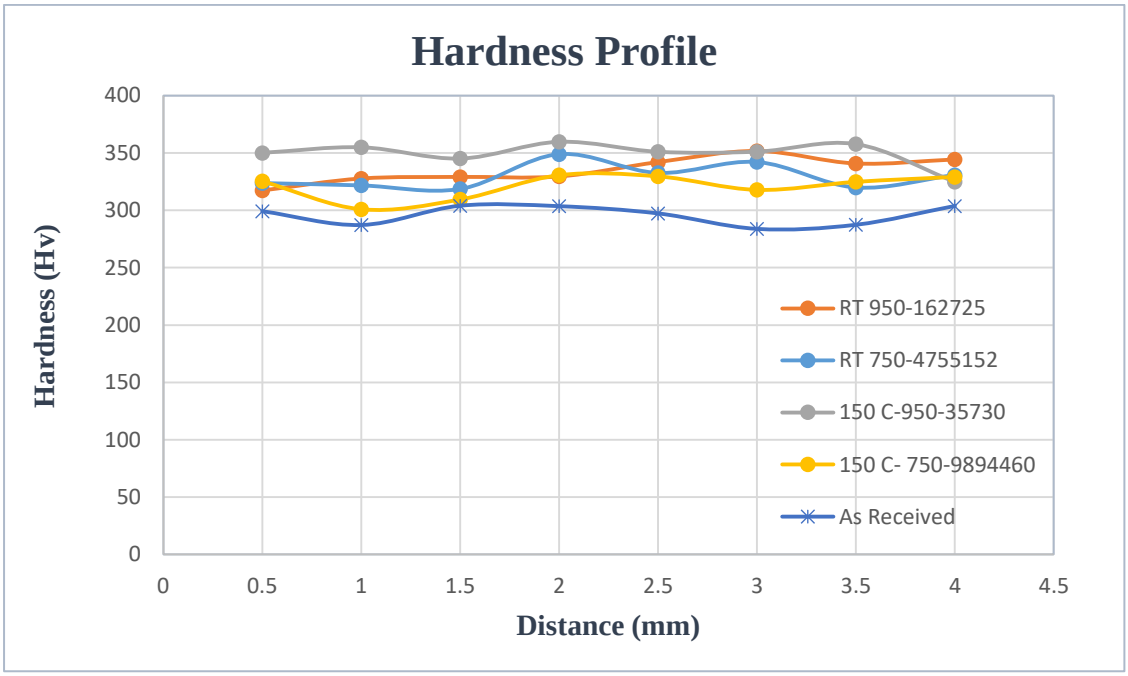


Fig 4.8: Hardness Profile of as received specimen and tested samples

The above graph showing the hardness of as received specimen and fatigue tested specimen.

The hardness of fatigue tested specimen is seen to be increasing on account of dynamic strain ageing.

Fatigue cycling can cause grain boundary strengthening by increasing dislocation pile-up at boundaries, which enhances resistance to plastic deformation.

The increase in hardness after fatigue testing is largely due to strain hardening, microstructural refinement, and dislocation interactions induced by cyclic loading.

# Chapter 5

# CONCLUSIONS

The constant amplitude fatigue behaviour of Ti 64 alloy at room temperature (RT) and 150 °C was studied, based on the research work carried out, following conclusions can be drawn:

1. The fatigue life reduced at 150 °C as compared to room temperature, primarily due to thermal activation of deformation mechanism and microstructural changes. At moderately elevated temperature thermal energy increases the mobility of dislocation within the material. This leads to easier initiation and propagation of micro-cracks under cyclic loading, reducing fatigue resistance.
2. At higher stress level 900 MPa for 150 °C temperature a drop in fatigue life was observed by 92% as compared to room temperature, whereas at lower stress level there is not much effect of the temperature
3. From the optical micrographs, it can be seen that the microstructure consisted of equiaxed grains. Alpha (α) light region and beta (β) dark region were seen on the structure.
4. Microstructure after fatigue testing showed fine grains due to dynamic strain ageing.
5. The fractrography of a failed specimen for RT shows brittle type of failure observed and crack in initiating from surface of the specimen, whereas for 150°C multiple crack initiating sites was observed at the surface.
6. The hardness of fatigue tested specimen was seen increasing, due to dynamic strain ageing and refinement in microstructure.

# Scope of future research

Future research should examine the effects on factors including

1. Variable loading
2. Temperature cycling
3. The fatigue characteristics
4. Attempt to more precisely model these complicated situations

# REFERENCES


[1] Zhihong Wua, “Microstructural effects on the high-cycle fatigue and fracture behaviors of Ti-6Al-4V alloy”, Engineering Fracture Mechanics 235 (2020) 107129

[2] G.Q. Wua, “Effect of microstructure on the fatigue properties of Ti–6Al–4V titanium alloys”, Materials and Design 46 (2013) 668–674

[3] K. Tokaji, “High cycle fatigue behaviour of Ti–6Al–4V alloy at elevate temperatures”, Scripta Materialia 54 (2006) 2143–2148

[4] R.J. Morrissey, “Frequency and stress ratio effects in high cycle fatigue of Ti–6Al–4V,” International Journal of Fatigue 21 (1999) 679–685

[5] G. Ellwood. Dieter and D. J. Bacon, *Mechanical metallurgy*. McGraw-Hill, 1988.

[6] “Introduction to aerospace materials,” in *Introduction to Aerospace Materials*, Elsevier, 2012, pp. 1–14. doi: 10.1533/9780857095152.1.

[7] Hung Dang Nguyen,” A Critical review on additive manufacturing of Ti-6Al-4V alloy: microstructure and mechanical properties,”Journal of Materials Research and Technology 2022. 18: 4641-4661

[8] Z. C. Luo, “Revealing the Fracture Mechanism of Twinning-Induced Plasticity Steels,” *Steel Res Int*, vol. 89, no. 9, Sep. 2018, doi: 10.1002/srin.201700433.

[9] “Mechanical Behaviour of Engineering Materials.”

[10] O. Savin *et al*, “Damage due to start-stop cycles of turbine runners under high-cycle fatigue under high-cycle fatigue,” *Int J Fatigue*, vol. 2021, doi: 10.1016/j.ijfatigue.2021.106458ï

[11] S. Kale *et al.*, “High-Temperature Fatigue Behaviour of Alloy 617M,” *Transactions of the Indian National Academy of Engineering*, vol. 7, no. 2, pp. 685–688, Jun. 2022, doi: 10.1007/s41403-022-00321-7.